

Investigation of the collapse of the skewness and kurtosis exhibited in atmospheric dispersion data (*)

D. M. LEWIS (**), P. C. CHATWIN and N. MOLE

*Applied Mathematics Section, School of Mathematics and Statistics
University of Sheffield - Sheffield, S3 7RH, UK*

(ricevuto il 10 Gennaio 1996; revisionato l'8 Luglio 1996; approvato il 23 Settembre 1996)

Summary. — This paper studies the collapse of the estimators for skewness and kurtosis of concentration onto a near universal curve. This phenomenon is observed for data taken from atmospheric dispersion experiments under a variety of different conditions. By means of careful investigation of the high concentration tails, modelled by means of the generalized Pareto distribution, and the fundamental physics of the problem, a set of envelope curves encompassing the data will be established. The implications of these results for modelling the probability density function of concentration are discussed.

PACS 92.60.Ek – Convection, turbulence, and diffusion.

PACS 92.60.Sz – Air quality and air pollution.

PACS 01.30.Cc – Conference proceedings.

1. – Introduction

Dispersion of gas assumed to be acting as a passive scalar (*i.e.* its chemical properties are unchanged on release and it has no effect on the velocity field) is governed by the equation

$$(1) \quad \frac{\partial \Gamma}{\partial t} + \nabla \cdot (\mathbf{u}\Gamma) = \kappa \nabla^2 \Gamma,$$

where $\Gamma(\mathbf{x}, t)$ is the concentration at position \mathbf{x} and time t , $\mathbf{u}(\mathbf{x}, t)$ is the velocity field (given by the Navier-Stokes equations) and κ the molecular diffusivity. Computing resources are as yet insufficient to accurately estimate the statistical properties such as the probability density function (pdf) of Γ by direct numerical simulation [1], and hence the formulation of simple models (based on physics) is of great importance.

(*) Paper presented at EUROMECH Colloquium 338 “Atmospheric Turbulence and Dispersion in Complex Terrain” and ERCOFTAC Workshop “Data on Turbulence and Dispersion in Complex Atmospheric Flows”, Bologna, 4-7 September 1995.

(**) Currently at: Dept. of Mathematics, City University, Northampton Square, London EC1V 0HB, UK.

One such model of Chatwin and Sullivan [2], based on a simple extension of the hypothetical case $\kappa = 0$, postulated the following relationship between the concentration mean $\mu(\mathbf{x}, t)$ and variance $\sigma^2(\mathbf{x}, t)$, namely

$$(2) \quad \sigma^2 = \beta^2 \mu(\alpha C_0 - \mu),$$

where C_0 is a local scale concentration for μ (e.g. the plume centreline mean concentration), and α and β are constants (see also Mole [3]). The authors demonstrated the applicability of this theory in the case of passive scalar dispersion in self-similar turbulent shear flows, although for the general case one would expect α and β to vary with position and time [4, 5]. They also postulated extending this theory for the higher moments of S (skewness) and K (kurtosis)

$$(3) \quad S = \frac{E\{(\Gamma - \mu)^3\}}{\sigma^3} = A_3 \frac{(\alpha - 2C)}{\{C(\alpha - C)\}^{1/2}},$$

$$(4) \quad K = \frac{E\{(\Gamma - \mu)^4\}}{\sigma^4} = A_4 \frac{(\alpha^2 - 3\alpha C + 3C^2)}{C(\alpha - C)},$$

where $C = \mu/C_0$, and A_3 and A_4 are constants of proportionality. It follows from (3) and (4) that

$$(5) \quad K = A_4 \left[\frac{S^2}{A_3^2} + 1 \right].$$

In [2] it was argued that $A_n^{1/n}$ is of $O(1)$. Mole and Clarke [6] studied the approximation $A_3 = A_4 = 1$, in which case

$$(6) \quad K = S^2 + 1$$

independent of the values of α and β , and suggested (6) would provide a simple test as to whether the theory of [2] is consistent with experimental evidence. Estimates of S and K calculated from measurements of concentration taken during continuous releases of contaminant over long periods of time are shown on fig. 1. These experiments were all assumed to be statistically stationary and the estimates for the moments shown here taken to be time-independent variables. The values collapse (to within experimental error) onto a quadratic curve of the form $K = AS^2 + B$ [6-8], close to but clearly above $K = S^2 + 1$. (In fact it is easy to prove [6, 9] that $K \geq S^2 + 1$ with equality if and only if the sample space consists of two points).

Further evidence of this phenomenon was exhibited in [6] with reference to the potential for harm expressed as a non-dimensional dosage, namely

$$(7) \quad D(\mathbf{x}, t; \rho, T) = \frac{1}{T} \int_{t-T/2}^{t+T/2} [\Gamma(\mathbf{x}, t')/\theta_s]^\rho dt',$$

where θ_s is the uniform source concentration, T is the exposure time and ρ a parameter characteristic of the gas. Dosage estimates of S and K for many different T and ρ values all fell very close to a single quadratic curve (e.g. fig. 3 of [6]). Subsequent investigation of data collected from a series of repetitions of a non-stationary, instantaneous release of heavy gas into a wind tunnel [7, 8], (where the evolution of the

moments with time was calculated by averaging over the repeats) has also highlighted a similar quadratic relationship between estimates of K and S (e.g. fig. 5 and 6 of [7]). These results demonstrate the wide applicability of this collapse and, although not directly considered here, provide further motivation for this work.

2. - Experiments and data sets

Details of the various field experiments, which are the sources of the data shown on fig. 1, are summarized in table I. All the data sets were pre-processed, to deal with noise and other instrument effects, using the maximum entropy inversion technique [10], where the performance of the ultra-violet ion collectors (UVICs) is also discussed.

The New Mexico site was basically flat for many kilometres and covered with intermittent scrub less than 0.4 m high. An ion source, 3 m above the ground, was positioned 5–15 m upwind of an array of detectors at heights between 3 and 3.5 m. Two experiments took place in the daytime (unstable conditions), and two at night (stable

TABLE I. - *Layout and weather conditions of the various field trials which are the sources of the data sets studied in this paper.*

Number and description of field trials	Four separate continuous steady release	Five separate continuous steady releases	Three separate continuous steady releases	FLADIS a single continuous steady release
Location	New Mexico	Dugway, Utah	Dugway, Utah	Landskrona, Sweden
Date	November 89	November 92	May 93	August 93
Tracer gas	Ionised air	Propylene	Propylene	Liquefied NH ₃
Detector used	Ion collectors	UVIC	UVIC	UVIC
Number of detectors	4	1	6	9
Downwind distance	15 m over a variety of configurations	30 m on plume centreline	20 m, split 2 m across plume	5 at 140 m, split 20 m across plume. 4 at 240 m at heights 0.5–10 m
Stability conditions	Two unstable Two stable	All neutral	All neutral	Stable
Mean windspeed	2–4 ms ⁻¹	0.8–2.9 ms ⁻¹	2.5 ms ⁻¹	3.2 ms ⁻¹
Sampling frequency	10 Hz	200 Hz	100 Hz	100 Hz
Duration of release	1800–3300 s	900 s	300 s	1200 s

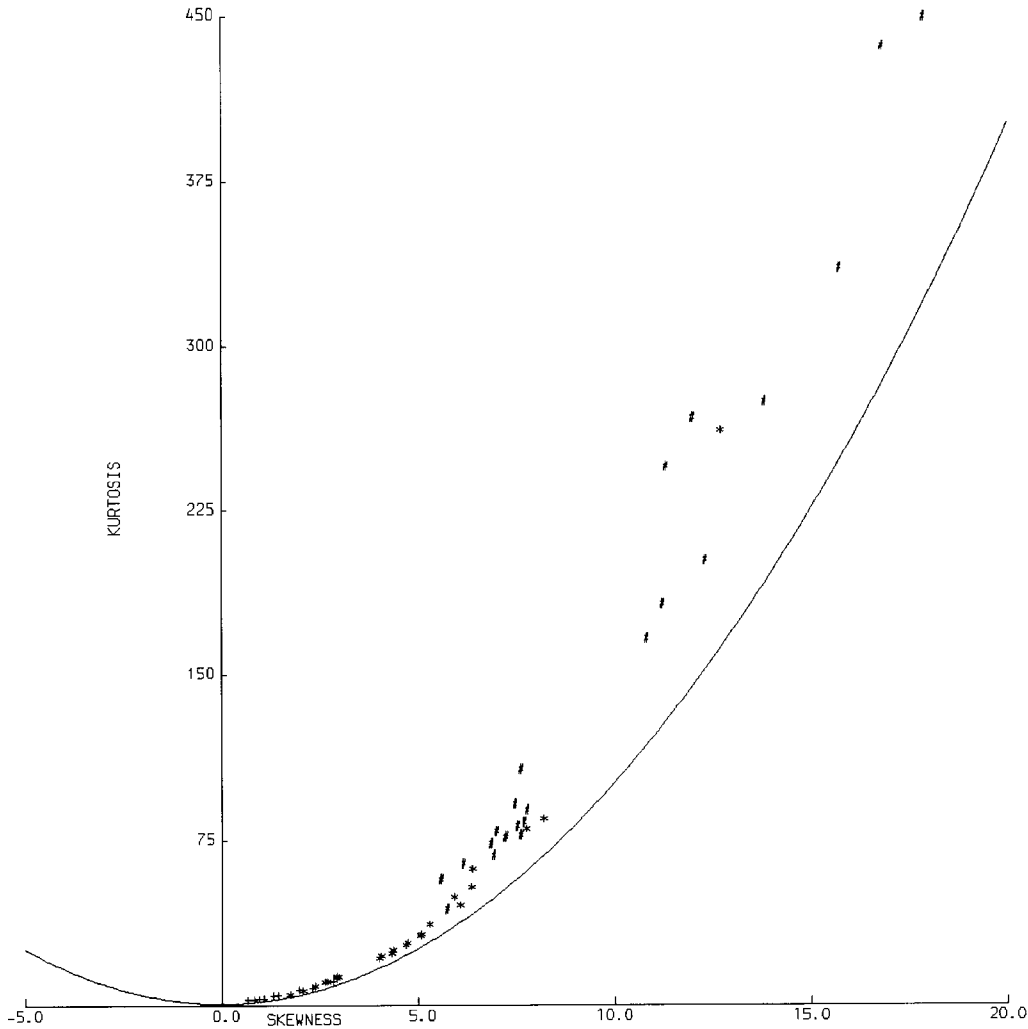


Fig. 1. - Plot of kurtosis vs. skewness for the various data sets described in the text. + FLADIS (stable) data; # Dugway (neutral) Nov. 92 and May 93; * New Mexico (unstable and stable). The solid line represents the curve $K = S^2 + 1$ which pertains to a two-state model.

conditions). These experiments, including performance of the ion collectors, are discussed in more detail in [11].

During the Dugway experiments propylene was released from a height of 1.32 m at a rate of $1.38 \times 10^{-4} \text{ m}^3 \text{ s}^{-1}$ (November 1992), and from 2 m at a rate of $2.5 \times 10^{-4} \text{ m}^3 \text{ s}^{-1}$ (May 1993), towards the array of UVICs positioned 2 m above the ground. The experiments were conducted by Jones [12], and further details are available from the authors.

The Landskrona experiments formed part of the EU FLADIS project [13] and took place over flat grassland (roughness height ~ 0.04 m). Ammonia was released from the source, fixed at a height of 1.5 m, at a near constant rate of approximately 0.27 kg s^{-1} .

The first array of detectors (fixed 2 m high) was spread across the plume. A second array further downwind was positioned approximately on the plume centreline at different heights.

The general characteristics of the output recorded by the detectors during these experiments are discussed in [14]. All exhibited positively skewed distributions to some degree (see fig. 1), with those recorded under neutral conditions (corresponding to the most intermittent data sets) producing the largest values.

3. - Analysis

The pdf of concentration $\rho(\theta; \mathbf{x}, t)$ is defined to be

$$(8) \quad \rho(\theta; \mathbf{x}, t) \delta\theta = PROB\{\theta \leq \Gamma(\mathbf{x}, t) < \theta + \delta\theta\}.$$

In terms of the pdf the central moments about the distribution mean $\mu(\mathbf{x}, t) = \mu_1$ are given by

$$(9) \quad \mu_n(\mathbf{x}, t) = \int_0^\infty \{\theta - (1 - \delta_{1n}) \mu_1(\mathbf{x}, t)\}^n \rho(\theta; \mathbf{x}, t) d\theta, \quad n \geq 1,$$

with variance $\sigma^2(\mathbf{x}, t) = \mu_2$, skewness $S = \mu_3 / \mu_2^{3/2}$ and kurtosis $K = \mu_4 / \mu_2^2$. In the absence of molecular diffusion Γ can take just two values, namely zero and θ_s , the uniform source concentration, and the pdf has the exact form of the weighted sum of two delta functions [2, 14]. The skewness and kurtosis of such a distribution satisfy $K = S^2 + 1$ exactly. As the higher moments in the real case $\kappa \neq 0$ lie on a similar $K = AS^2 + B$ characteristic curve, one could consider modelling the concentration pdf as a perturbation of a two-state process, namely

$$(10) \quad \rho(\theta; \mathbf{x}, t) = \{1 - \varepsilon(\mathbf{x}, t)\} \rho_L(\theta; \mathbf{x}, t) + \varepsilon(\mathbf{x}, t) \rho_T(\theta; \mathbf{x}, t),$$

where $\rho_L(\theta; \mathbf{x}, t)$ and $\rho_T(\theta; \mathbf{x}, t)$ are themselves pdfs and $\varepsilon(\mathbf{x}, t) \in [0, 1]$ is a shape parameter. For such a pdf it is possible to show [15] that

$$(11) \quad \mu = (1 - \varepsilon) \mu_L + \varepsilon \mu_T,$$

$$(12) \quad \sigma^2 = \varepsilon \sigma_T^2 + (1 - \varepsilon) \sigma_L^2 + \varepsilon(1 - \varepsilon) \phi^2,$$

$$(13) \quad S\sigma^3 = (1 - 2\varepsilon)(1 - \varepsilon) \varepsilon \phi^3 + 3\varepsilon(1 - \varepsilon) \phi(\sigma_T^2 - \sigma_L^2) + (1 - \varepsilon) S_L \sigma_L^3 + \varepsilon S_T \sigma_T^3,$$

$$(14) \quad K\sigma^4 = \varepsilon(1 - \varepsilon)(1 - 3\varepsilon + 3\varepsilon^2) \phi^4 + 6\varepsilon(1 - \varepsilon)[\varepsilon \sigma_L^2 + (1 - \varepsilon) \sigma_T^2] \phi^2 + \\ + 4\phi \varepsilon(1 - \varepsilon)(S_T \sigma_T^3 - S_L \sigma_L^3) + (1 - \varepsilon) \sigma_L^4 K_L + \varepsilon \sigma_T^4 K_T,$$

where $\phi = \mu_T - \mu_L$ and the subscripts T and L refer to the moments of ρ_T and ρ_L , respectively.

Just such a model pdf has been used successfully to fit statistically stationary atmospheric dispersion data sets [14], with

$$(15) \quad \rho_L(\theta; \mathbf{x}) = \frac{e^{-\theta/\lambda}}{\lambda(1 - H(\zeta) e^{-v/\lambda\zeta})}$$

a simple exponential distribution to model the low concentration peak, and a generalized Pareto distribution (GPD)

$$(16) \quad p_T(\theta; \mathbf{x}) = \frac{1}{\nu} \left(1 - \frac{\zeta\theta}{\nu} \right)^{1/\zeta - 1}$$

to model the high concentration tails [16,17]. $\lambda(\mathbf{x}) > 0$ and $\nu(\mathbf{x}) > 0$ represent appropriate concentration scales, $H(\zeta)$ a Heaviside step function and $\zeta(\mathbf{x})$ is a shape parameter determining the range of θ . For $\zeta > 0$, then $0 < \theta < \nu/\zeta$, in which case all the moments exist, whilst for $\zeta \leq 0$, $0 < \theta < \infty$ and the μ_n exist only when $\zeta > -1/n$. (The case $\zeta = 0$ is interpreted as the limit $\zeta \rightarrow 0$.) The parameters λ , ε and ζ were chosen using a maximum likelihood procedure, and the scale parameter ν was simultaneously chosen to minimize the discrepancies among the first four sample and fitted central moments [14]. This ensures that $\zeta > -1/4$; otherwise K is not defined. In practice, the likelihood function was relatively insensitive to changes in ν and adopting this procedure reduced its value by less than 1 per cent. The pdf must terminate at some maximum value $\leq \theta_S$, so the case $\zeta \leq 0$ is unphysical. However, as better fits to the data were obtained by adopting the procedure described above with $\zeta > -1/4$, and given that it is difficult to make a robust estimate of the maximum concentration, the restriction that $\zeta > 0$ was not imposed. In practice $\zeta \in (-1/5, 1/2)$ with $\zeta > 0$ for the Landskrona and New Mexico [18] data, whilst for the Dugway data $\zeta < 0$.

Using distributions (15) and (16) and noting that the normalizing factor $e^{-\nu/\lambda\zeta}$ is sufficiently small to be redundant ($e^{-\nu/\lambda\zeta} < 10^{-10}$ for all the data sets), one has

$$(17) \quad \mu_L = \lambda, \quad \sigma_L = \lambda, \quad S_L = 2, \quad K_L = 9.$$

$$(18) \quad \begin{cases} \mu_T = \frac{\nu}{(1+\zeta)}, & \sigma_T = \frac{\nu}{(1+\zeta)(1+2\zeta)^{1/2}}, \\ S_T = \frac{2(1-\zeta)(1+2\zeta)^{1/2}}{(1+3\zeta)}, & K_T = \frac{3(2\zeta^2 - \zeta + 3)(1+2\zeta)}{(1+3\zeta)(1+4\zeta)}. \end{cases}$$

Assuming that the values of the scale parameters are such that the condition $\mu_T \gg \mu_L$ is satisfied, then eqs. (12), (13) and (14) for the variance, skewness and kurtosis become

$$(19) \quad \sigma^2 = \frac{2\nu^2\varepsilon}{(1+\zeta)(1+2\zeta)} \left[1 - \frac{\varepsilon(1+2\zeta)}{2(1+\zeta)} \right],$$

$$(20) \quad S\sigma^3 = \frac{6\nu^3\varepsilon}{(1+\zeta)(1+2\zeta)(1+3\zeta)} \left[1 - \frac{\varepsilon(1+3\zeta)}{(1+\zeta)} + \frac{\varepsilon^2(1+2\zeta)(1+3\zeta)}{3(1+\zeta)^2} \right],$$

$$(21) \quad K\sigma^4 = \frac{24\nu^4\varepsilon}{(1+\zeta)(1+2\zeta)(1+3\zeta)(1+4\zeta)} \times \\ \times \left[1 - \frac{\varepsilon(1+4\zeta)}{(1+\zeta)} + \frac{\varepsilon^2(1+3\zeta)(1+4\zeta)}{2(1+\zeta)^2} - \frac{\varepsilon^3(1+2\zeta)(1+3\zeta)(1+4\zeta)}{8(1+\zeta)^3} \right].$$

A relationship of the form $K \approx AS^2 + B$ can be derived from (19), (20) and (21) by defining A and B correct for $O(\varepsilon^{-1})$ and $O(\varepsilon^0)$. The size of the error term $\Delta = K - AS^2 - B$ introduced when adopting this procedure can also be investigated. Following the routine algebra discussed in the appendix, one can show that

$$(22) \quad K = AS^2 + B + \Delta,$$

where

$$(23) \quad A = \frac{4(1 + 3\zeta)}{3(1 + 4\zeta)},$$

$$(24) \quad B = \frac{3(1 + 2\zeta)^2}{(1 + 3\zeta)(1 + 4\zeta)},$$

and

$$(25) \quad \Delta = K - AS^2 - B = \frac{(1 + 2\zeta)^2 \varepsilon}{2(1 + \zeta)(1 + 3\zeta)(1 + 4\zeta)} \frac{\left[1 - \frac{(2 + 3\zeta) \varepsilon}{2(1 + \zeta)} + \frac{(1 + 2\zeta)(2 + 3\zeta) \varepsilon^2}{12(1 + \zeta)^2} \right]}{\left[1 - \frac{(1 + 2\zeta) \varepsilon}{2(1 + \zeta)} \right]^3},$$

for $\zeta \in (-1/4, \infty)$. Differentiating (25) with respect to ε , one can show that, for each fixed ζ , Δ takes its maximum value

$$(26) \quad \Delta_{\text{MAX}} = \frac{(2 + \zeta)(1 + 2\zeta)^2}{3(1 + 3\zeta)(1 + 4\zeta)}$$

as $\varepsilon \rightarrow 1$ from below. Notice that $\Delta_{\text{MAX}} < 2/3$ for $\zeta \in (0, 3/2 + \sqrt{7/2})$. Furthermore, $\Delta \rightarrow 0$ as $\zeta \rightarrow \infty$, provided $\varepsilon < 1$.

4. - Discussion

4.1. Using a GPD model with $\zeta \geq 0$. - The previous analysis shows that using a GPD to model the high concentration tails implies a relationship between the skewness and kurtosis of the form (22)-(24), provided the error term (25) is sufficiently small. With no molecular diffusion $\varepsilon = \gamma(\mathbf{x}, t) < 1$, where γ is the intermittency factor [19], $\rho_L(\theta) = \delta(\theta)$ and $\rho_T(\theta) = \delta(\theta_S - \theta)$. This case is recovered from (15) and (16) by taking the limits $\lambda \rightarrow 0$ and $\zeta \rightarrow \infty$, with $\lim_{\zeta \rightarrow \infty} (\nu/\zeta) = \theta_S$. (In [20] a simplified three-parameter EGPd pdf model is described in which λ and ν are defined in terms of ε , ζ and μ the mean concentration, in such a way that $\rho_L(\theta) \rightarrow \delta(\theta)$ and $\rho_T(\theta) \rightarrow \delta(\theta_S - \theta)$ as $\zeta \rightarrow \infty$.) These limits give $A \rightarrow 1$, $B \rightarrow 1$ and $\Delta \rightarrow 0$ and one recovers from (22) the $K = S^2 + 1$ behaviour associated with two delta functions.

In practice the effects of molecular diffusion are to reduce concentration scales and smooth out associated concentration fluctuations [2, 19], introducing a continuum of observed concentration values. Generally for the experiments considered here the concentration data consists mainly of small measurements close to zero, interspersed

TABLE II. – Typical values of the parameters characterising the model pdf discussed in this paper for data collected under different atmospheric conditions.

Experiment	ε	μ_L/μ_T	$(1 - \varepsilon) \sigma_L^2/\varepsilon\sigma_T^2$
FLADIS stable data	0.55	0.011	1.2×10^{-4}
	0.88	0.074	1.4×10^{-3}
	0.36	0.033	2.3×10^{-3}
New Mexico unstable data	0.12	0.018	2.9×10^{-3}
	0.22	9.3×10^{-3}	3.5×10^{-4}
	0.13	0.018	2.0×10^{-3}
Dugway 93 neutral data	0.05	3.4×10^{-3}	1.6×10^{-4}
	0.12	8.3×10^{-3}	3.2×10^{-4}
	0.20	7.8×10^{-3}	1.6×10^{-4}
Dugway 92 neutral data	0.29	0.040	7.6×10^{-3}
	0.27	0.053	4.8×10^{-3}
	0.27	0.064	6.1×10^{-3}

with intermittent high value peaks [14]. After fitting the proposed model pdf to the data sets, all the scale parameters satisfied the $\mu_T \gg \mu_L$ criterion (see table II) and, hence, the analysis of the previous section is applicable. Except possibly very close to the source, one would expect the gradient of a real pdf to be finite at the maximum observed concentration. For this model this condition is satisfied only when $\zeta \leq 1/2$, and hence one can postulate that $\zeta = 1/2$ should provide an upper bound on the shape parameter. For the higher moments this would imply that the skewness and kurtosis satisfy

$$(27) \quad K \geq \frac{10}{9} S^2 + \frac{8}{5}.$$

(This lower bound on K is not invalidated by the error term, since $\Delta > 0$ for $\zeta > 0$.) The curve $K = 10/9 S^2 + 8/5$ is the lowest of the three shown on fig. 2 and, as anticipated, all the data points lie above it.

A number of special cases can be considered. When $\zeta \rightarrow 0$ the GPD deforms to an exponential distribution and the central moments of all orders exist. In this case $\Delta_{\text{MAX}} = 2/3$ and the skewness and kurtosis lie approximately on the curve

$$(28) \quad K = \frac{4}{3} S^2 + 3,$$

(see the middle curve shown on fig. 2). The best least squares fit of the moments generally lies close to this curve [6]. Notice how for the data collected under stable conditions the moments tend to lie below this curve, whilst under more convective conditions the moments are much larger (this is a consequence of the more intermittent structure of the data, which for this model manifests itself in smaller values of the parameter ε) and lie above it. Further special cases such as the gamma and lognormal [6] and beta [21] distributions have also been considered.

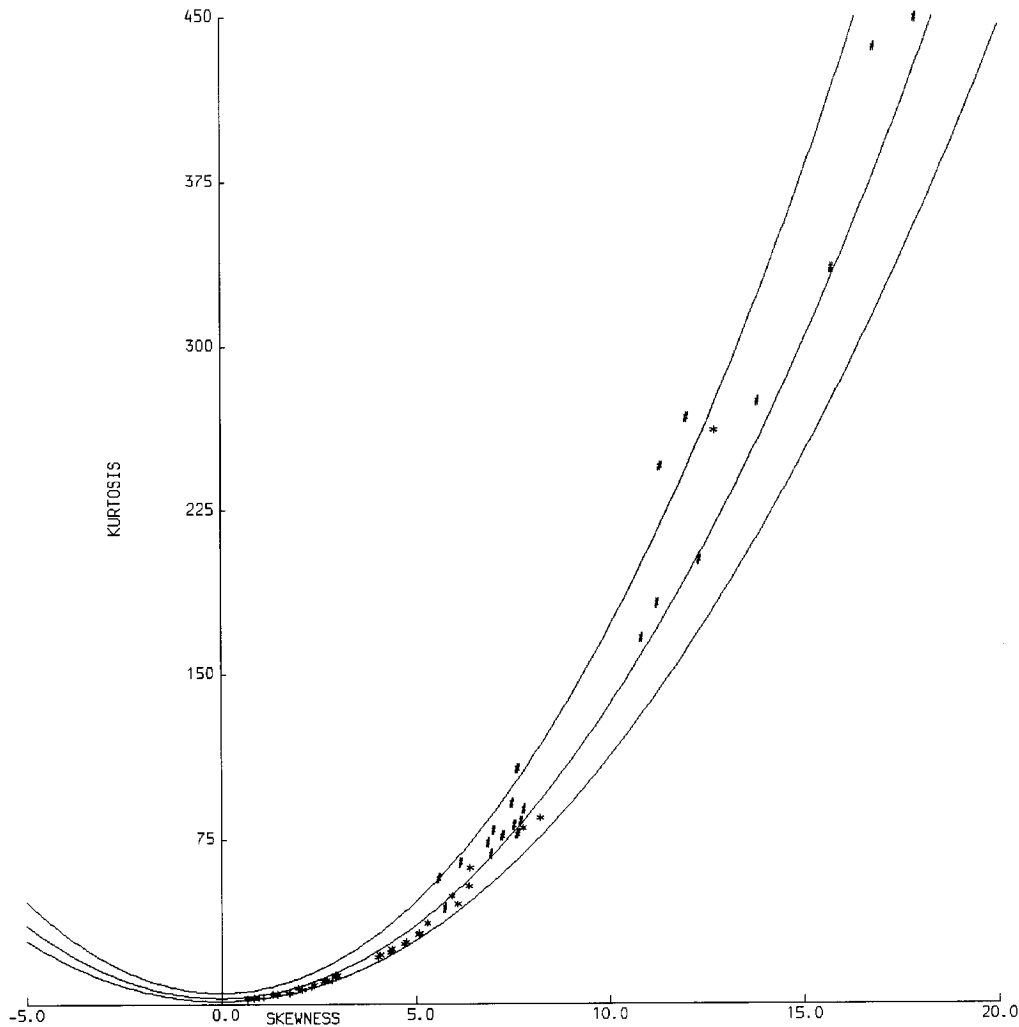


Fig. 2. - Plot of kurtosis vs. skewness for the various data sets described in the text. + FLADIS (stable data); # Dugway (neutral) Nov. 92 and May 93; * New Mexico (unstable and stable). The solid lines represent the theoretical curves $K = 5S^2/3 + 27/5$ (upper), $K = 4S^2/3 + 3$ (middle) and $K = 10S^2/9 + 8/5$ (lower). Little confidence can be placed in the data points lying above $K = 5S^2/3 + 27/5$.

4.2. *Using a GPD model with $\zeta < 0$.* - As can be seen from fig. 2, a number of points lie above $K = 4S^2/3 + 3$, implying negative ζ values. As was pointed out in sect. 3 such a pdf does not terminate, at odds with the fundamental physical property that Γ must be less than the source concentration. However, much better fits for the Dugway data based on the likelihood criterion are obtained by allowing $\zeta < 0$. The fitting procedure gives $\zeta \in (-1/5, 0)$, whilst the associated standard errors of ζ range from 1.5 to 3.4×10^{-4} . However, these errors assume independent time series, whilst the estimated autocorrelation time scale for these data sets is about 0.5 s. Block averaging the data

over intervals of 1 s to produce a series of independent data points resulted in fitted values of $\zeta > -0.1$ with much larger standard errors of order 3.5×10^{-2} , although these are still too small to be consistent with a $\zeta > 0$ distribution.

Further insight into the behaviour of the normalized moments in such circumstances can be gained by examining the theoretical standard error estimates of S and especially K , assuming that Γ is taken from a distribution with $\zeta < 0$. Using standard statistical results [7], it is possible to obtain (see appendix) an approximate expression (A.14) for variance of the estimator \widehat{K} , when ζ is slightly greater than $-1/8$. Notice that when ε is small, corresponding to large values of K (see eqs. (19) and (21)) as is the case for the Dugway data (table II), large standard errors can be expected. This is consistent with the bootstrap estimates of Clarke [22] for the confidence intervals of S and K , which show greatest uncertainty for large K . Calculations of the error (A.14) for the block-averaged Dugway data with $N = 900$ independent data points showed that $[\text{Var}(\widehat{K})]^{1/2}/\widehat{K} \sim 2$, too large to draw firm conclusions. The possibility that all of the points lying above $K = 4/3 S^2 + 3$ on fig. 2 were drawn from a $\zeta > 0$ GPD distribution (consistent with physical arguments) cannot be ruled out, although this is at odds with the error estimates on ζ from the likelihood fitting procedure. The resolution of this contradiction must await further data, in which there is more confidence in the estimates of the larger concentrations.

4.3. General case. – For general $p_L(\theta)$ and $p_T(\theta)$ then, provided $\mu_T \gg \mu_L$ and $\varepsilon \sigma_T^2 \gg (1 - \varepsilon) \sigma_L^2$ (in which case $\sigma_T^2 \gg \sigma_L^2$ and it is reasonable to assume $S_T \sigma_T^3 \gg S_L \sigma_L^3$ and $K_T \sigma_T^4 \gg K_L \sigma_L^4$ from (9)) one can show from (12)–(14) that

$$(29) \quad S^2 \approx \frac{[S_T + 3(1 - \varepsilon) \omega + (1 - 2\varepsilon)(1 - \varepsilon) \omega^3]}{\varepsilon[1 + (1 - \varepsilon) \omega^2]^3},$$

$$(30) \quad K \approx \frac{[K_T + 4(1 - \varepsilon) S_T \omega + 6(1 - \varepsilon)^2 \omega^2 + (1 - \varepsilon)(1 - 3\varepsilon + 3\varepsilon^2) \omega^4]}{\varepsilon[1 + (1 - \varepsilon) \omega^2]^2},$$

where $\omega = \mu_T/\sigma_T$. (The constraint $\varepsilon \sigma_T^2 \gg (1 - \varepsilon) \sigma_L^2$ appears characteristic of this data on the evidence of the GPD fits displayed in table II.) The analysis outlined in the appendix will hold and $K = AS^2 + B + \Delta$, with constants A and B given by equations (A.3) and (A.4), respectively. However, it is not clear that the resultant error term, Δ , is sufficiently small to be neglected, as was the case for the GPD pdf discussed earlier. Further investigation is being undertaken. It is also difficult to make progress by letting $\varepsilon \rightarrow 0$ and expanding, without introducing further constraints on the behaviour of ω , S_T and K_T . Ye [23] has proposed a model pdf for wind tunnel data consisting of a weighted sum of two Gaussian distributions, but with $\sigma_T = \sigma_L$, in which case (29), (30) do not apply. One can show that for such a pdf the normalized moments satisfy the relationship $K = S^2 + B$, but this is too restrictive to account for all the data discussed here.

5. – Conclusions

The collapse of the normalized moments, skewness and kurtosis, for concentration and dosage onto a characteristic quadratic curve, irrespective of the experimental or atmospheric conditions, must imply certain common features shared by the pdfs.

Appeals to the basic physics of the problem of atmospheric dispersion in the light of these results support the proposition that the pdf of concentration can be modelled as a perturbation of a two-state process. Examination of the results of specific experiments investigating the continuous release of contaminant (under statistically stationary conditions) shows that such a pdf, consisting of an exponential distribution and GPD, can be used successfully to model the data. Furthermore, it has been shown (to a good approximation) that it is the characteristics of the GPD alone that govern the behaviour of the higher moments, leading to $K = A(\zeta) S^2 + B(\zeta)$ consistent with the observed collapse. The resultant error term Δ introduced has the elegant property of taking its maximum value as $\epsilon \rightarrow 1$ from below, for each fixed ζ , and $\Delta < 2/3$ for $\zeta \in (0, 3/2 + \sqrt{7}/2)$. Physical arguments suggest that ζ should be limited to positive values; although some of the data does support the idea of negative values. However, in these instances the data in the high concentration tail is too sparse to make robust estimates of S and K .

Following on from this work, it is possible to postulate further improvements to the model pdf. Whilst ζ is dependent on atmospheric conditions ($\zeta < 0$ for data collected in neutral conditions, $0 < \zeta < 1/2$ for stable/unstable conditions), it shows little variation (except very close to the source) with respect to \mathbf{x} , the relative position of the detectors to the source, *i.e.* the estimated values of skewness and kurtosis, from data recorded at different positions during a single experiment, lie (approximately) on a single curve. This would imply the use of a model pdf defined by eqs. (10), (15), (16) with ζ constant for continuous releases under fixed atmospheric conditions. Furthermore, by applying the arguments deployed here concerning the relative size of the concentration scale parameters, *i.e.* $\mu_T \gg \mu_L$, one can postulate a simple relationship between the mean and variance which reduces to three only the number of independent parameters governing the pdf [20], simplifying the model still further. Given that the $(\widehat{S}, \widehat{K})$ collapse is also characteristic of data taken from non-stationary instantaneous release experiments [8, 9], the GPD should be considered as a starting point for a simple model pdf evolving with time.

* * *

We wish to thank W. ZIMMERMAN and L. CLARKE for their helpful comments and discussions. This work has been carried out with the support of the Chemical and Biological Defence Establishment (CBDE). We also gratefully acknowledge the help of Drs. D. RIDE and C. JONES of the CBDE for the provision of the various experimental data sets.

APPENDIX

Derivation of A, B and Δ

Using eqs. (29) and (30), which represent a general form of eqs. (19)-(21), as a starting point, and assuming that to a first approximation the skewness and kurtosis satisfy $K = AS^2 + B$, one has

$$\begin{aligned} \text{(A.1)} \quad \epsilon^{-1} [K_T + 4(1 - \epsilon) S_T \omega + 6(1 - \epsilon)^2 \omega^2 + (1 - \epsilon)(1 + 3\epsilon + 3\epsilon^2) \omega^4] [1 + (1 - \epsilon) \omega^2] = \\ = A\epsilon^{-1} [S_T + 3(1 - \epsilon) \omega + (1 - 2\epsilon)(1 - \epsilon) \omega^3]^2 + B[1 + (1 - \epsilon) \omega^2]^3. \end{aligned}$$

Rearranging (A.1) gives

$$(A.2) \quad [(K_T + 4S_T\omega + 6\omega^2 + \omega^4)\varepsilon^{-1} - 4\omega(S_T + 3\omega + \omega^3) + 6\varepsilon\omega^2(1 + \omega^2) - 3\varepsilon^2\omega^4][(1 + \omega^2) - \varepsilon\omega^2] = \\ = A\varepsilon^{-1}[(S_T + 3\omega + \omega^3) - 3\varepsilon\omega(1 + \omega^2) + 2\varepsilon^2\omega^3]^2 + B[(1 + \omega^2) - \varepsilon\omega^2]^3.$$

If $\rho_T(\theta)$ follows a GPD, then $\omega = (1 + 2\zeta)^{1/2}$ and the results given by eq. (18) for S_T and K_T apply. As the moments of $\rho_T(\theta)$ are independent of ε , it is possible to determine expressions for A and B by assuming $K = AS^2 + B$ is correct for $O(\varepsilon^{-1})$ and $O(\varepsilon^0)$. Equating terms of $O(\varepsilon^{-1})$ in (A.2) \Rightarrow

$$(A.3) \quad A = \frac{[K_T + 4S_T\omega + 6\omega^2 + \omega^4](1 + \omega^2)}{[S_T + 3\omega + \omega^3]^2},$$

whilst equating terms of $O(\varepsilon^0)$ \Rightarrow

$$(A.4) \quad B = \frac{\omega[S_T + 3\omega + \omega^3](6A - 4)}{(1 + \omega^2)^2} - \frac{\omega^2[K_T + 4S_T\omega + 6\omega^2 + \omega^4]}{(1 + \omega^2)^3}.$$

For a GPD (A.3) and (A.4) reduce to

$$(A.5) \quad A = \frac{4(1 + 3\zeta)}{3(1 + 4\zeta)},$$

$$(A.6) \quad B = \frac{3(1 + 2\zeta)^2}{(1 + 3\zeta)(1 + 4\zeta)},$$

and hence one obtains eqs. (22)-(24).

The error term introduced by adopting this strategy can be examined by evaluating $\Delta = K - AS^2 - B$, with A and B as given by equations (A.3) and (A.4). Equation (A.2) represents $[(1 + \omega^2) - \varepsilon\omega^2]^3 K = [(1 + \omega^2) - \varepsilon\omega^2]^3 (AS^2 + B)$ and so taking all the terms onto the LHS of this equation and noting the terms $O(\varepsilon^{-1})$ and $O(\varepsilon^0)$ are zero by (A.3) and (A.4), one has

$$(A.7) \quad [(1 + \omega^2) - \varepsilon\omega^2]^3 \Delta = \varepsilon[4\omega^3(S_T + 3\omega + \omega^3)(1 - A) + 3\omega^2(1 + \omega^2)^2(2 + B - 3A)] + \\ + \varepsilon^2[3\omega^4(1 + \omega^2)(4A - B - 3)] + \varepsilon^3[\omega^6(3 + B - 4A)].$$

For a GPD the LHS of (A.7) gives

$$(A.8) \quad [(1 + \omega^2) - \varepsilon\omega^2]^3 \Delta = 8(1 + \zeta)^3 \left[1 - \frac{\varepsilon(1 + 2\zeta)}{2(1 + \zeta)} \right]^3 \Delta,$$

whilst using (18), (A.5) and (A.6), the terms on the RHS of (A.7) in ε , ε^2 and ε^3 reduce to

$$(A.9) \quad \varepsilon \frac{4[(1 + \zeta)(1 + 2\zeta)]^2}{(1 + 3\zeta)(1 + 4\zeta)},$$

$$(A.10) \quad -\varepsilon^2 \frac{2(1 + \zeta)(1 + 2\zeta)^2(2 + 3\zeta)}{(1 + 3\zeta)(1 + 4\zeta)},$$

and

$$(A.11) \quad \varepsilon^3 \frac{(1 + 2\zeta)^3(2 + 3\zeta)}{3(1 + 3\zeta)(1 + 4\zeta)},$$

respectively. Substituting results (A.8)-(A.11) into (A.7) and rearranging gives the equation for the error term (25).

Variance of \widehat{K}

For large samples of N independent data points, the variance of the kurtosis measure $\widehat{K} = m_4/m_2^2$, where

$$(A.12) \quad m_r = \frac{1}{N} \sum_{j=1}^N (\bar{\Gamma}_j - \bar{\Gamma})^r,$$

is given by (see exercise 10.27 of [9])

$$(A.13) \quad \text{Var}(\widehat{K}) = \frac{1}{N\mu_2^3} \left[\frac{\mu_8}{\mu_2} - 4 \frac{\mu_6\mu_4}{\mu_2^2} + 4 \frac{\mu_4^3}{\mu_2^3} - \frac{\mu_4^2}{\mu_2} + 16 \frac{\mu_4\mu_3^2}{\mu_2^2} - 8 \frac{\mu_3\mu_5}{\mu_2} + 16\mu_3^2 \right].$$

Given the relative size of the concentration scales ($\nu \gg \lambda$) for the pdf described here, the central moments appearing in (A.13) will be dominated by the contribution of the GPD. In this case all moments exist only when $\zeta > -1/8$. As $\zeta \rightarrow -1/8$ from above, only the first term in (A.13) is significant and it reduces to

$$(A.14) \quad \text{Var}(\widehat{K}) \sim \frac{2520 [(1 + \zeta)(1 + 2\zeta)]^3}{\varepsilon^3 (1 + 3\zeta)(1 + 4\zeta) \dots (1 + 8\zeta) N} \left[1 - \frac{\varepsilon(1 + 2\zeta)}{2(1 + \zeta)} \right]^{-4}.$$

(Note that $\text{Var}(\widehat{K})$ is not defined for $\zeta \leq -1/8$. The curve $K = 5/3 S^2 + 27/5$ corresponding to $\zeta = -1/8$ in (22)-(24) is the upper curve shown in fig. 2.)

REFERENCES

[1] CHATWIN P. C. and SULLIVAN P. J., *Boundary-Layer Meteorol.*, **62** (1993) 269.
 [2] CHATWIN P. C. and SULLIVAN P. J., *J. Fluid Mech.*, **212** (1990) 533.
 [3] MOLE N., *Environmetrics*, **6** (1995) 559.
 [4] SAWFORD B. L. and SULLIVAN P. J., *J. Fluid Mech.*, **289** (1995) 141.
 [5] CLARKE E. D. and MOLE N., *Environmetrics*, **6** (1995) 607.
 [6] MOLE N. and CLARKE E. D., *Boundary-Layer Meteorol.*, **73** (1995) 35.
 [7] ZIMMERMAN W. B. and CHATWIN P. C., *Boundary-Layer Meteorol.*, **75** (1995) 321.
 [8] CHATWIN P. C. and ROBINSON C., *this issue*, p. 361.
 [9] STUART A. and ORD J. K., in *Kendall's Advanced Theory of Statistics*, Vol. **1**, *Distribution Theory*, 6th edition (Edward Arnold, London) 1994, pp. 108-122 and 346-373.
 [10] LEWIS D. M. and CHATWIN P. C., *Boundary-Layer Meteorol.*, **72** (1995) 53.

- [11] MOLE N. and JONES C. D., *Boundary-Layer Meteorol.*, **67** (1994) 41.
- [12] JONES C. D., personal communication.
- [13] NIELSEN M., BENGTSOON R., JONES C. D., NYRÉN K., OTT S. and RIDE D. J., in *Design of the FLADIS Field Experiments with Dispersion of Liquefied Ammonia*, Risø National Laboratory, Roskilde, Denmark, 1994.
- [14] LEWIS D. M. and CHATWIN P. C., *Environmetrics*, **6** (1995) 583.
- [15] CHATWIN P. C., LEWIS D. M. and MOLE N., *Math. Comput. Modell.*, **21** (1995) 11.
- [16] DAVISON A. C. and SMITH R. L., *J. R. Stat. Soc.*, **52**, No. 3 (1990) 393.
- [17] SMITH R. L., *Stat. Sci.*, **4**, No. 4 (1989) 367.
- [18] MOLE N., ANDERSON C. W., NADARAJAH S. and WRIGHT C., *Environmetrics*, **6** (1995) 595.
- [19] CHATWIN P. C. and SULLIVAN P. J., *Phys. Fluids A*, **1**, No. 4 (1989) 761.
- [20] LEWIS D. M. and CHATWIN P. C., *J. Appl. Meteorol.*, **36** (1997) 1064.
- [21] CHATWIN P. C., LEWIS D. M. and SULLIVAN P. J., *Environmetrics*, **6** (1995) 395.
- [22] CLARKE E. D., in *Probabilistic models of gaseous dispersion*, PhD Thesis, University of Sheffield, Sheffield, England (1996).
- [23] YE H., in *A new statistic for the contaminant dilution process in turbulent flows*, PhD Thesis, University of Western Ontario, London, Ontario, Canada (1995).